Microsc. Microanal. 19, 507–512, 2013
doi:10.1017/S143192761300038X

Microscopy AND Microanalysis

Single Particle Tracking Analysis of the Chloroplast Division Protein FtsZ Anchoring to the Inner Envelope Membrane

Carol B. Johnson,[1,†] Leung K. Tang,[2,†] Aaron G. Smith,[2,3] Akshaya Ravichandran,[1] Zhiping Luo,[4,5] Stanislav Vitha,[4] and Andreas Holzenburg[1,2,4,*]

[1]*Department of Biology, Texas A&M University, College Station, TX 77843-3258, USA*
[2]*Department Biochemistry and Biophysics, Texas A&M University, College Station, TX 77843-2128, USA*
[3]*Department of Structural Biology, University of Pittsburgh, Pittsburgh, PA 15260, USA*
[4]*Microscopy and Imaging Center, Texas A&M University, College Station, TX 77843-2257, USA*
[5]*Department of Chemistry and Physics, Fayetteville State University, Fayetteville, NC 28301, USA*

Abstract: Replication of chloroplast in plant cells is an essential process that requires co-assembly of the tubulin-like plastid division proteins FtsZ1 and FtsZ2 at mid-chloroplast to form a ring structure called the Z-ring. The Z-ring is stabilized via its interaction with the transmembrane protein ARC6 on the inner envelope membrane of chloroplasts. Plants lacking ARC6 are defective in plastid division and contain only one or two enlarged chloroplasts per cell with abnormal localization of FtsZ: instead of a single Z-ring, many short FtsZ filaments are distributed throughout the chloroplast. ARC6 is thought to be the anchoring point for FtsZ assemblies. To investigate the role of ARC6 in FtsZ anchoring, the mobility of green fluorescent protein–tagged FtsZ assemblies was assessed by single particle tracking in mutant plants lacking the ARC6 protein. Mean square displacement analysis showed that the mobility of FtsZ assemblies is to a large extent characterized by anomalous diffusion behavior (indicative of intermittent binding) and restricted diffusion suggesting that besides ARC6-mediated anchoring, an additional FtsZ-anchoring mechanism is present in chloroplasts.

Key words: ARC6, FtsZ anchoring, chloroplast division, *Arabidopsis thaliana*, particle tracking, anomalous diffusion

Introduction

Chloroplasts evolved as a result of an endosymbiotic event between a free-living photosynthetic cyanobacterium and a nonphotosynthetic eukaryote (Douglas, 1998; Martin & Herrmann, 1998; McFadden, 1999). Chloroplasts and other types of plastids replicate via binary fission to maintain adequate cellular levels during cell proliferation (Leech et al., 1981; Osteryoung & Nunnari, 2003). This binary fission is initiated by two nuclear-encoded plastid-targeted homologs of the bacterial cell division protein FtsZ (Osteryoung & Vierling, 1995; Osteryoung, 2000; Osteryoung & McAndrew, 2001; Miyagishima et al., 2004). Plants harbor two distinct FtsZ protein families, FtsZ1 and FtsZ2, both of which are required for normal plastid division. The division process is initiated by co-assembly of FtsZ1 and FtsZ2 into a ring structure (Z-ring) at the division site (Vitha et al., 2001), which then recruits other chloroplast division proteins to assemble a functional division machinery both in the chloroplast stroma and on the outer, cytosolic side of the chloroplast envelope membrane. Among the chloroplast division proteins, ARC3 and ARC6 play a pivotal role in the regulation of Z-ring assembly and localization. ARC3 interacts with FtzZ1 and together with PARC6 (Glynn et al., 2009) regulates proper positioning of the division site (Maple et al., 2007). On the other hand, the integral inner-envelope membrane protein ARC6 interacts with FtsZ2. In the absence of ARC6, FtsZ forms numerous short filaments throughout the chloroplast instead of a single Z-ring (McAndrew et al., 2001; Vitha et al., 2003), and it was suggested that ARC6 anchors the Z-ring to the envelope membrane of the chloroplast (Glynn et al., 2008). Here we test this hypothesis by analyzing the mobility of FtsZ assemblies in plants lacking ARC6, i.e., the *arc6* mutant (Pyke et al., 1994; Vitha et al., 2003).

Materials and Methods

All *Arabidopsis thaliana* plants used in the experiments are in the ecotype Wassiljevskija background, greenhouse-grown at a temperature of 22°C and a relative humidity of 62%. Wild-type (WT) and *arc6* mutant seeds were obtained from Arabidopsis Biological Resource Center at Ohio State University, Columbus, OH, USA. *Agrobacterium*-mediated plant transformation was performed as described (Clough & Bent, 1998), using plasmids conferring glufosinate resistance as a selectable marker and containing *A. thaliana FtsZ1-1* or *FtsZ2-1* constructs with the appropriate native promoter and encoding the full length FtsZ1 or FtsZ2 proteins with a green fluorescent protein (GFP) tag at the C-terminus (Vitha et al., 2001). T1 seedlings were selected by spraying with 120 mg/L glufosinate ammonium as a selection agent. Stable, nonsegregating transgenic lines were

Received December 12, 2012; accepted January 31, 2013
**Corresponding author*. E-mail: holzen@tamu.edu
[†]These authors contributed equally to this work.

then identified in subsequent generations and used for experiments.

Extracts from expanding leaves from approximately 5-week-old plants were prepared, separated by SDS-PAGE, and transferred to nitrocellulose membranes as described by Stokes et al. (2000). The relative amount of total protein was measured by densitometry of a Coomassie-stained gel, using ImageJ software. The amount of extract was then adjusted accordingly in subsequent gel runs to ensure equal gel loading. Extract from approximately 1-mg fresh tissue was loaded per lane. Immunoblotting was performed essentially as described by Stokes et al. (2000). The anti-FtsZ1 antibody (McAndrew et al., 2001) was used at 1:10,000 dilution overnight at 4°C. For detection of FtsZ2, affinity purified goat anti-peptide antibody, recognizing the residues 168 through 184 in FtsZ2-1 (Stokes et al., 2000), was custom prepared by Alpha Diagnostics (San Antonio, TX, USA), diluted 1:25 in TBST containing 0.25% (v/v) cold water fish gelatin, and used for 3 h at room temperature. Rabbit anti-goat IgG, horseradish peroxidase-conjugate secondary antibody (Millipore, Billerica, MA, USA) was used at 1:10 000 dilution in TBST containing 0.25% (v/v) cold water fish gelatin. Blots were developed using SuperSignal West Pico Chemiluminescent Substrate Kit (Thermo Scientific, Portsmouth, NH, USA), and the signal was recorded on Blue X-Ray Film (Phenix Research Products, Candler, NC, USA). Equal loading was confirmed by Ponceau S staining of the RuBisCO band on membranes [0.1% (w/v) Ponceau S in 5% (v/v) acetic acid]. Densitometry of FtsZ bands was performed from scanned films, using the Gel Analyzer tool in the ImageJ v1.47 freeware (http://imagej.nih.gov/ij/).

Segments from young, rapidly expanding leaves were excised, mounted in perfluorodecalin (Littlejohn et al., 2010), and viewed using a Olympus FV1000 confocal microscope (Olympus, Tokyo, Japan) equipped with a 60×/1.2 water immersion objective. Zoom and image size were adjusted to achieve 0.1 μm per pixel sampling. Time lapse image series of 200 frames were recorded with 0.5-s frame intervals and analyzed using ImageJ software (http://rsb. info.nih.gov/ij) and the SpotTracker plugin (Sage et al., 2005). The generated tracking coordinates were subsequently used to calculate the mean square displacement (MSD; Saxton & Jacobson, 1997).

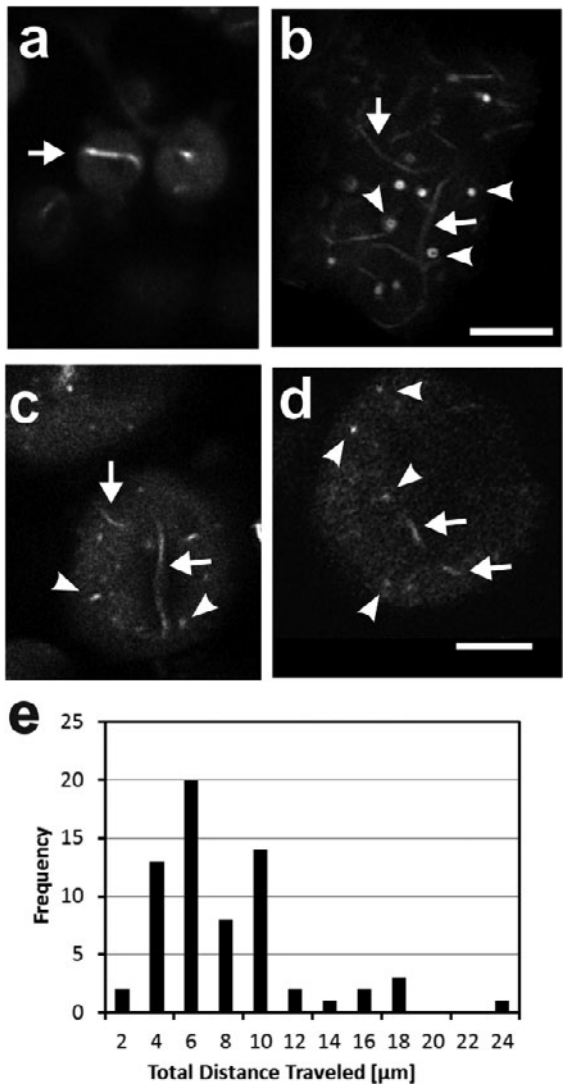

Figure 1. FtsZ-GFP localization and mobility in chloroplasts. (**a–d**) Fluorescence micrographs of FtsZ-GFP localization in chloroplasts. (**a**) FtsZ1-GFP in WT background. The FtsZ ring is indicated by an arrow. (**b**) FtsZ2-GFP in WT background. The enlarged chloroplasts contain both FtsZ filaments (arrows) and mini-rings or puncta (arrowheads). (**c**) FtsZ1-GFP and (**d**) FtsZ2-GFP in the *arc6* mutant background again highlighting short filaments and puncta. (**e**) Distribution of total distances traveled by puncta in the *arc6* background over time (100 s). Scale bars, 5 μm.

Results

Transgenic plants of WT background exhibited mostly filamentous assemblies of FtsZ-GFP. In plants with expression levels of the GFP-tagged FtsZ1 up to twofold over that of the native expression levels in WT plants as based on quantitative Western blot analysis, the GFP signal was observed as a ring (Z-ring) at mid plastid (Fig. 1a). With FtsZ2-GFP at comparable expression levels in the WT background—while generally showing a similar localization pattern—an additional feature could be observed: the localization to mini-rings or puncta (Fig. 1b). These puncta were often too small to be resolved as ring-like structures using diffraction-limited fluorescence microscopy but could be identified as rings by super-resolution microscopy (data not shown). Compared to the WT-background plants, the localization pattern of FtsZ-GFP in plants lacking the ARC6 protein (*arc6* mutant) was different. Both FtsZ1-GFP and FtsZ2-GFP formed multiple short filaments as well as puncta, and Z-rings were absent (Figs. 1c, 1d). This observation was consistent with previously reported immunofluorescence localization of FtsZ in the *arc6* mutant (Vitha et al., 2003). Since FtsZ1 and FtsZ2 have been shown to co-localize in the *arc6* as well as in other *arc* mutants (McAndrew et al., 2001), fluorescence microscopy of either of the two GFP-tagged proteins provides localization for both FtsZ1 and FtsZ2.

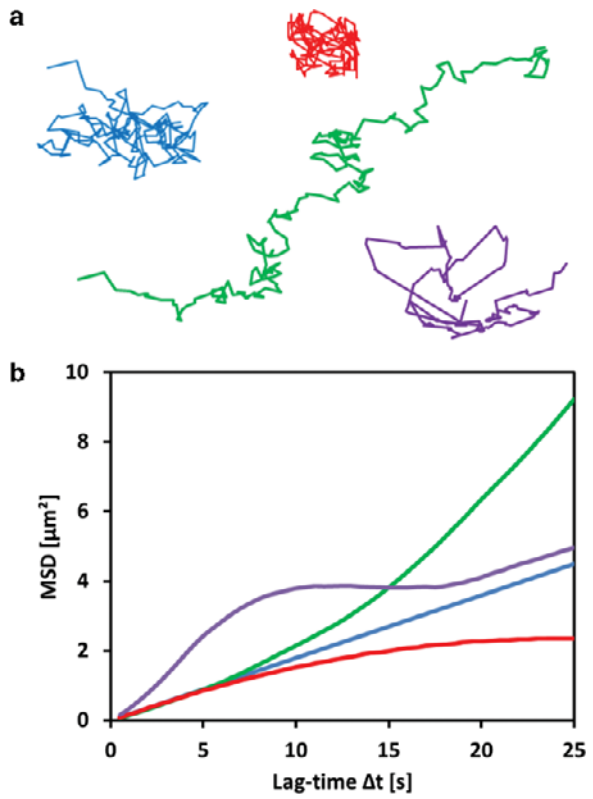

Figure 2. Movement pattern classification using X, Y trajectories and MSD plots. (**a**) Particle trajectories and (**b**) MSD plots reveal different diffusion modes. (**a**) From left to right: free (blue), confined (red), directed (green), and anomalous diffusion (purple). (**b**) MSD plots for the trajectories shown in panel **a**.

To quantify the mobility of FtsZ puncta, single particle tracking (SPT) was employed. When tracking structures over time, the original thought was that the total distance traveled (Fig. 1e) could be an indicator as to whether a structure was mobile or stationary with the total distance traveled asymptotically approaching zero for stationary objects. However, both freely diffusing and small membrane-anchored structures are subject to Brownian motion, and their stochastic movements constantly add to the traveling distance making it impossible to deduce the degree of mobility from the distance traveled. The histogram of the total distance traveled in Figure 1e shows an approximately normal distribution with a mean of 7 ± 2.7 μm and a small peak toward larger distances (>14 μm). For the data in the main peak, there is no correlation between distance traveled and the diffusion mode, and they can therefore not be used to differentiate between mobile and stationary behavior in line with the argument above. However, for the data outside the main distribution, i.e., in the small peak toward larger distances (>14 μm), there is a correlation inasmuch as all those puncta have intermittent binding in common (see Fig. 2).

To differentiate between mobile and nonmobile punctate structures, the calculation and analysis of MSD over time is a more appropriate tool (Saxton & Jacobson, 1997). It also permits estimating diffusion coefficients and allows further characterization of the movement or, more specifically, the diffusion mode (see below). When analyzing X, Y trajectories (Fig. 2a) using MSD plots, one can deduce the diffusion mode from the shape and slope of the curves as shown in Figure 2b. The categorical dissection of movements leads to a differentiation into the following four modes: free, directed, confined (also known as restricted), and anomalous diffusion. Free diffusion plots follow the form MSD (μm^2) $= 4D\,\Delta t$ for a two-dimensional analysis (X, Y) with D being the diffusion coefficient and Δt the lag time. For directed diffusion, this changes to the quadratic term $4D\,\Delta t + v^2\Delta t^2$ with v being the mean velocity and with confined diffusion, the MSD plot reaches a plateau (maximum μm^2 value) for larger lag times (Δt). Anomalous diffusion as observed in this study was more modulated than suggested by MSD (μm^2) $= 4D\Delta t^n$ with $n < 1$ following plain subdiffusive behavior (Ruthardt et al., 2011) and appears to harbor two discrete states: a mobile state and a confined one. This gives rise to an overall shape of the curve that could be described as a smoothed step function. For the purpose of the study, it was most important to differentiate between mobility and nonmobility. To this end, mobile puncta would be exhibiting free (isotropic random walk) or directed diffusion while puncta showing confined or anomalous diffusion would be classified as nonmobile. Anomalous patterns are indicative of intermittent binding and can therefore be readily differentiated from the free diffusion/isotropic random walk or directed diffusion curve characteristics for mobile puncta.

In the actual measured datasets (with $n = 69$ from 15 different chloroplasts and 10 different plants), both FtsZ1-GFP and FtsZ2-GFP established the same mobility pattern, which is consistent with co-localization and co-assembly of FtsZ1 and FtsZ2 *in vivo*. The trajectories and MSD plots are summarized in Figure 3, and examples are given for the diffusion scenarios typically encountered. Thirty percent of the cases clearly belonged to the mobile fraction showing free diffusion (Fig. 3a), while 70% would fall in either the confined diffusion (Fig. 3b) or anomalous diffusion mode (Figs. 3c–3f) constituting intermittent binding. The ratio between confined movement and intermittent binding was approximately 2:1. The anomalous diffusion/intermittent binding mode can be made up of a combination of different diffusion behaviors and typically a confined mode is encountered in combination with free or directed diffusion. The latter is demonstrated in more detail for the X, Y trajectory in Figure 3e, which was subjected to subtrajectory analysis (Figs. 3g, 3h) as it could be broken down into two distinct subregions. The first part of the trajectory exhibits confinement (Figs. 3e, 3g, red) before the tracked object takes off in an accelerated manner toward the second subregion where it starts slowing down at the very end (Figs. 3e, 3h, green). The intermittent binding mode in Figure 3c is likely to consist of free and confined diffusion with the MSD plot curving downward indicating that the object is returning back toward the point where the first frame ($t = 0$; point of origin) was measured. In Figure 3d, the MSD plot indicates

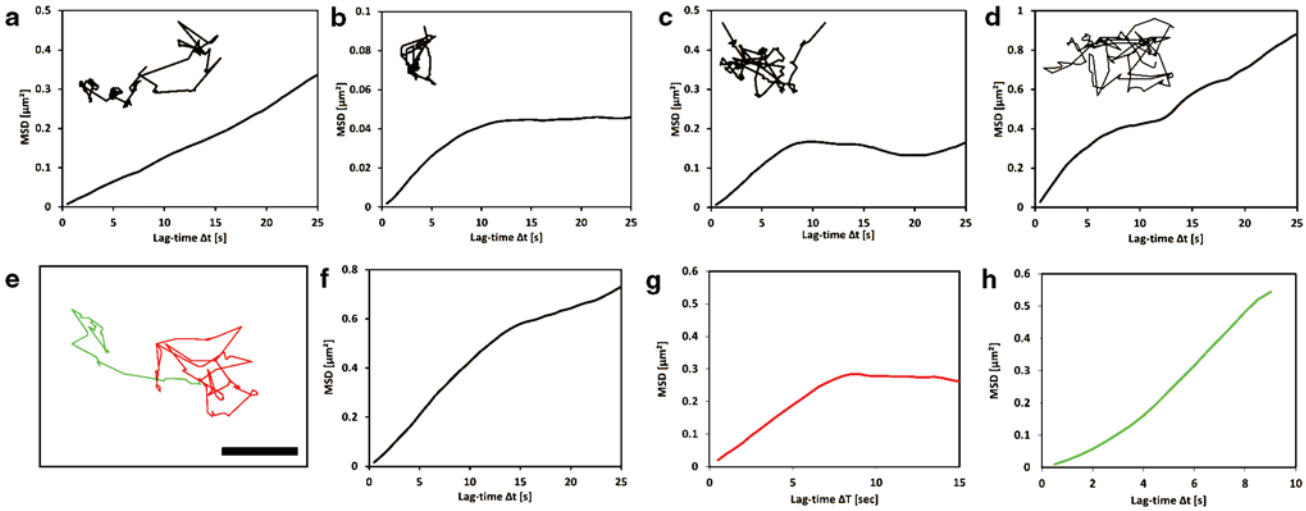

Figure 3. Representative X, Y trajectories and MSD plots for FtsZ-GFP puncta in the *arc6* background. (**a**) Free, (**b**) restricted, and (**c**, **d**) anomalous diffusion modes. The trajectory in panel **e** reveals a combination of confined (red) and predominantly directed diffusion (green) as apparent from the MSD plots showing the (**f**) entire trajectory in conjunction with the subtrajectories from frames taken at (**g**) 0–61.5 s and (**h**) 62–100 s. The scale bar in panel **e** corresponds to 2 μm.

that the object may be intermittently moving away from the point of origin.

In comparison with the *arc6* mutant plants, it was expected that in the WT background the FtsZ assemblies would be less mobile. While spot tracking was not feasible in plants expressing FtsZ1-GFP due to the exclusive presence of long filaments (see also below), plants expressing FtsZ2-GFP exhibited trackable small annular or punctate structures. MSD analysis of 27 datasets (originating from eight different chloroplasts) revealed intermittent binding in 30% of the cases, while confined diffusion constituted the remaining 70% of the datasets. No instances of free diffusion were observed. These data are in agreement with the expected confinement or anchoring of FtsZ in the presence of ARC6.

Visual inspection of all the tracked datasets confirmed that the spot tracking algorithm worked reliably on the punctate FtsZ assemblies. The images were of sufficient signal-to-noise ratio, and since the imaging was performed with a point-scanning confocal microscope in conjunction with short integration times (2 μs/pixel), dynamic errors (Ruthardt et al., 2011)—typically arising from particles diffusing within the integration time of a camera and leading to localization uncertainties and smearing—do not appear to have compromised the robustness of our datasets.

In addition to tracking the FtsZ puncta, an attempt was made to analyze the mobility of the filamentous assemblies. It was found that the precision in tracking was lacking behind the one experienced with the puncta. The tracking software employed is designed for spot analysis while tracking of elongated features is subjected to more uncertainties. In addition, if and when filament movements were observed, these movements could be of a different level of complexity typically characterized by tumbling, flailing, as well as twirling and twisting on a spot with little or no

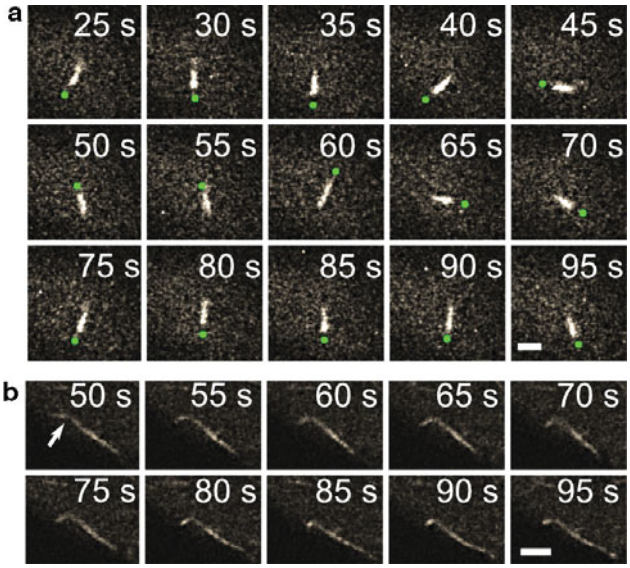

Figure 4. Mobility of short FtsZ-GFP filaments in the *arc6* background. Frame sequences at the indicated time points. (**a**) A pirouette-like movement is depicted with one end of the filament marked (green dot) for ease of orientation. The filament in panel **b** highlights the development of a flexibly hinged terminal region (arrow at $t = 50$ s). Scale bars, 2 μm.

translational movement such as the pirouette-like motions shown in Figure 4a. Furthermore, parts of otherwise stationary filaments could exhibit flailing from a short hinged region (Fig. 4b). Here it should be noted that the filament has been initially anchored along its entire length prior to the development of a flexibly hinged terminal region. Directional movements are typically absent from FtsZ filaments in the WT plants and were only occasionally observed in the *arc6* background amounting to less than 5% of the filaments ($n = 94$). In these rare cases the filaments would not

just simply perform a linear move but were moving while twirling around a central pivot point, i.e., translational movements were only observed in conjunction with rotations around an axis perpendicular to the length of the filament.

Discussion

At the onset of this work, it was predicted that in the absence of the presumed FtsZ anchor ARC6 (Vitha et al., 2003; Glynn et al., 2008), FtsZ assemblies would undergo free diffusion in the chloroplast stroma. This was not observed. In fact, the majority of FtsZ puncta exhibited confined diffusion or a combination of confined diffusion and free diffusion, indicative of intermittent binding, and pointing at an additional, ARC6-independent FtsZ anchor. Given the fact that in the absence of ARC6 FtsZ2 still interacts with FtsZ1 and that interactions between FtsZ1 and ARC3 as well as ARC3 and the inner-envelope membrane protein PARC6 have been reported (Maple et al., 2007; Glynn et al., 2009), it is possible that the ARC3-PARC6 complex constitutes the alternate anchor.

The movement of FtsZ puncta from one confinement area to another ("hopping") is consistent with the presence of FtsZ-anchoring sites throughout the chloroplast. For this hopping to occur, there has to be sufficient affinity between FtsZ and the anchoring sites as well as sufficient dissociation of FtsZ from the anchor either via an anchored FtsZ molecule releasing itself from the filament or from the anchor itself. Either case supports an enhanced on- and off-rate required for hopping. A rapid turnover of FtsZ molecules in and out of filamentous assemblies has been reported for plant FtsZ expressed in yeast (TerBush & Osteryoung, 2012). This is in line with the interpretation presented here that any interaction between the anchor and an individual FtsZ molecule is only temporary. In the absence of ARC6, the number or strength of the anchoring sites was not sufficient to completely confine the FtsZ puncta to one location. This was even more apparent in some of the filamentous assemblies analyzed, where the entire filament would initially be anchored, but then the filament end would become dissociated from its anchor and start flailing, while the rest of the filament remained essentially immobile.

The MSD analysis proved to be a useful tool in studying the diffusional behavior of the FtsZ puncta. However, some of the MSD curves indicated a complex mobility pattern that was not readily interpretable. Recently, new software tools for analysis of changes in particle movement behavior, such as transitions between Brownian motion and temporary confinement, were developed (Menchón et al., 2012) and will be of interest for further study of complex diffusional behavior.

Conclusions

Laser scanning confocal microscopy in conjunction with X,Y SPT and MSD analysis proved to be a useful tool for studying diffusional mobility of FtsZ in *A. thaliana* chloroplasts and revealed the presence of an ARC6-independent FtsZ anchoring mechanism. Both anchoring mechanisms are characterized by transient binding enabling hopping movements. This leads to MSD plots that fall into the anomalous diffusion category and produce curves that often take the shape of smoothed step functions.

Acknowledgments

The use of the Microscopy and Imaging Center facility at Texas A&M University is acknowledged. The Olympus FV1000 confocal microscope acquisition was supported by the Office of the Vice President for Research at Texas A&M University.

References

Clough, S.J. & Bent, A.F. (1998). Floral dip: A simplified method for *Agrobacterium*-mediated transformation of *Arabidopsis thaliana*. *Plant J* **16**, 735–743.

Douglas, S.E. (1998). Plastid evolution: Origins, diversity, trends. *Curr Opin Genet Dev* **8**, 655–661.

Glynn, J.M., Froehlich, J.E. & Osteryoung, K.W. (2008). *Arabidopsis* ARC6 coordinates the division machineries of the inner and outer chloroplast membranes through interaction with PDV2 in the intermembrane space. *Plant Cell* **20**, 2460–2470.

Glynn, J.M., Yang, Y., Vitha, S., Schmitz, A.J., Hemmes, M., Miyagishima, S.Y. & Osteryoung, K.W. (2009). PARC6, a novel chloroplast division factor, influences FtsZ assembly and is required for recruitment of PDV1 during chloroplast division in *Arabidopsis*. *Plant J* **59**, 700–711.

Leech, R.M., Thomson, W.W. & Platt-Aloia, K.A. (1981). Observations on the mechanism of chloroplast division in higher plants. *New Phytol* **87**, 1–9.

Littlejohn, G.R., Gouveia, J.D., Edner, C., Smirnoff, N. & Love, J. (2010). Perfluorodecalin enhances *in vivo* confocal microscopy resolution of *Arabidopsis thaliana* mesophyll. *New Phytol* **186**, 1018–1025.

Maple, J., Vojta, L., Soll, J. & Møller, S.G. (2007). ARC3 is a stromal Z-ring accessory protein essential for plastid division. *EMBO Rep* **8**, 293–299.

Martin, W. & Herrmann, R.G. (1998). Gene transfer from organelles to the nucleus: How much, what happens, and why? *Plant Physiol* **118**, 9–17.

McAndrew, R.S., Froehlich, J.E., Vitha, S., Stokes, K.D. & Osteryoung, K.W. (2001). Colocalization of plastid division proteins in the chloroplast stromal compartment establishes a new functional relationship between FtsZ1 and FtsZ2 in higher plants. *Plant Physiol* **127**, 1656–1666.

McFadden, G.I. (1999). Endosymbiosis and evolution of the plant cell. *Curr Opin Plant Biol* **2**, 513–519.

Menchón, S.A., Martin, M.G. & Dotti, C.G. (2012). APM_GUI: Analyzing particle movement on the cell membrane and determining confinement. *BMC Biophys* **5**, 4.

Miyagishima, S.Y., Nozaki, H., Nishida, K., Nishida, K., Matsuzaki, M. & Kuroiwa, T. (2004). Two types of FtsZ proteins in mitochondria and red-lineage chloroplasts: The duplication of FtsZ is implicated in endosymbiosis. *J Mol Evol* **58**, 291–303.

Osteryoung, K.W. (2000). Organelle division: Crossing the evolutionary divide. *Plant Physiol* **123**, 1213–1216.

Osteryoung, K.W. & McAndrew, R.S. (2001). The plastid division machine. *Annu Rev Plant Physiol Plant Mol Biol* **52**, 315–333.

Osteryoung, K.W. & Nunnari, J. (2003). The division of endosymbiotic organelles. Early divergence of the FtsZ1 and FtsZ2 plastid division gene families in photosynthetic eukaryotes. *Science* **302**, 1698–1704.

Osteryoung, K.W. & Vierling, E. (1995). Conserved cell and organelle division. *Nature* **376**, 473–474.

Pyke, K.A., Rutherford, S.M., Robertson, E.J. & Leech, R.M. (1994). *arc6*, a fertile *Arabidopsis* mutant with only two mesophyll cell chloroplasts. *Plant Physiol* **106**, 1169–1177.

Ruthardt, N., Lamb, D.C. & Brauchle, C. (2011). Single-particle tracking as a quantitative microscopy-based approach to unravel cell entry mechanisms of viruses and pharmaceutical nanoparticles. *Mol Ther* **19**, 1199–1211.

Sage, D., Neumann, F.R., Hediger, F., Gasser, S.M. & Unser, M. (2005). Automatic tracking of individual fluorescence particles: Application to the study of chromosome dynamics. *IEEE Trans Image Process* **14**, 1372–1383.

Saxton, M.J. & Jacobson, K. (1997). Single-particle tracking: Applications to membrane dynamics. *Annu Rev Biophys Biomol Struct* **26**, 373–399.

Stokes, K.D., McAndrew, R.S., Figueroa, R., Vitha, S. & Osteryoung, K.W. (2000). Chloroplast division and morphology are differentially affected by overexpression of *FtsZ1* and *FtsZ2* genes in *Arabidopsis*. *Plant Physiol* **124**, 1668–1677.

TerBush, A.D. & Osteryoung, K.W. (2012). Distinct functions of chloroplast FtsZ1 and FtsZ2 in Z-ring structure and remodeling. *J Cell Biol* **199**, 623–637.

Vitha, S., Froehlich, J.E., Koksharova, O., Pyke, K.A., van Erp, H. & Osteryoung, K.W. (2003). ARC6 is a J-domain plastid division protein and an evolutionary descendant of the cyanobacterial cell division protein Ftn2. *Plant Cell* **15**, 1918–1933.

Vitha, S., McAndrew, R.S. & Osteryoung, K.W. (2001). FtsZ ring formation at the chloroplast division site in plants. *J Cell Biol* **153**, 111–119.